ACS OMEGA

Article

Cite This: ACS Omega 2019, 4, 4691−4696

http://pubs.acs.org/journal/acsodf

New Polylactic Acid Multifunctional Ultrasound Contrast Agent Based on Graphene Oxide as the Carrier of Targeted Factor and Drug Delivery

Jie Zhang,*,† Limei Song,† Huiming Zhang,‡ Shujing Zhou,* Yufeng Jiao,† Xiangyu Zhang,† Yue Zhao,† and Ying Wang†

†School of Pharmacy and ‡School of Basic Medicine, Jiamusi University, Jiamusi 154007, China

ABSTRACT: In recent years, the development of ultrasound contrast agents has encouraged their use as a drug system for diagnosis and therapy. In this paper, polylactic acid (PLA) composite microbubbles (FA/DOX/GO/DOX/PLA) were prepared with graphene oxide (GO) as a carrier of the targeted factor folic acid (FA) and doxorubicin (DOX) by the multiple emulsification−solvent evaporating process. Appearance, particle size, and zeta potential of PLA composite microbubbles were characterized by using a nanoparticle size analyzer and transmission electron microscopy. Breast cancer cells MCF-7 were used to evaluate the antitumor activity of PLA composite microbubbles in vitro by using the CCK-8 and acridine orange staining method. The ultrasonic imaging effect of PLA composite microbubbles was investigated in New Zealand white rabbits by the Doppler color ultrasound imaging system. With Kunming mice as the research model, the acute toxicity of PLA composite microbubbles was examined. The experimental results showed that the prepared PLA composite microbubbles presented a hollow and spherical shape with a particle size of 600 nm or so and a zeta potential of −37.5 ± 10.0 mV. They had a good effect of the enhancing imaging, and clear ultrasound imaging can be obtained. PLA composite microbubbles showed a significant proliferation inhibition effect on breast cancer cells MCF-7 in a dose-dependent manner. After PLA composite microbubbles were modified by FA, they were good for targeting FA receptors on the surface of MCF-7 cells, which increased the inhibition rate of the tumor cells. LD_{50} of PLA composite microbubbles was 87.529 mg·kg^{-1}; the mice did not show the acute toxicity when the dose of composite microbubbles was lower than this value.

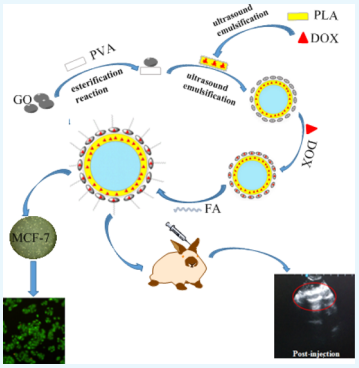

1. INTRODUCTION

Nowadays, malignant tumors are second only to cardiovascular disease in human health, among which breast cancer is a common cancer worldwide and it seriously affects the female body and life.[1,2] Early diagnosis and treatment is an important measure to improve the survival rate of cancer patients. Ultrasound contrast agents (UCAs) can enhance the contrast of ultrasound images in vivo by intravenous injection when ultrasound diagnosis is performed, thereby providing more basis for diagnosis and treatment of diseases.[3] The continuous development of new UCAs has encouraged their use in the diagnosis and treatment of cerebral perfusion,[4−6] breast tumor,[7] stomach cancer,[8] carotid artery, and ovarian cancer.[9−11]

Graphene oxide (GO) is a two-dimensional carbon nanomaterial with a large specific surface area, which has become a focus of attention as a drug carrier. GO can carry aromatic ring drugs through noncovalent interactions to achieve drug delivery in the body. Studies have generally found that GO possesses a large number of active groups such as carboxyl, carbonyl, hydroxyl, and epoxy groups. The existence of these groups is not only conducive to its biochemical structural modification but also makes it have good biocompatibility.[12]

With doxorubicin (DOX) as the model drug and GO modified with folic acid (FA) as the new biological material, the delivery system of polylactic acid (PLA) composite microbubbles was constructed and has been described in this paper. For this new composite microbubble UCA, the ultrasound imaging effect in vivo and in vitro, the inhibition of the breast cancer cells MCF-7 in vitro, and acute toxicity in Kunming (KM) mice were studied.

2. RESULTS AND DISCUSSION

2.1. Structure of the Targeting Drug-Loaded PLA Composite Microbubbles. As shown in Figure 1a, the microbubble film was constructed by using the GO-combined PLA; the drug was loaded not only on the GO but also within the microbubble with DOX as the model drug. Meanwhile, FA was used as the targeted factor and modified on the surface of the composite microbubble. It can be seen from transmission electron microscopy (TEM), as shown in Figure 1b, that the PLA composite microbubble showed a hollow structure, resulting from encasing N_2 inside the microbubble. GO was

Received: December 4, 2018
Accepted: February 7, 2019
Published: March 4, 2019

DOI: 10.1021/acsomega.8b03403
ACS Omega 2019, 4, 4691−4696

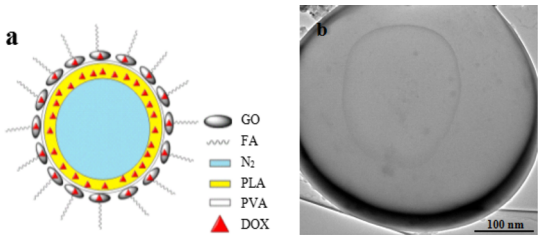

Figure 1. FA/DOX/GO/DOX/PLA microbubbles. (a) Structure simulation and (b) TEM.

linked on the surface of the composite microbubble; hence, the microbubble membrane layer appeared dark. Specifically, the introduced DOX during the preparation of the primary suspension sustained in the PLA film and the bonding product of GO and polyvinyl alcohol (PVA) was used as the film-forming agent and covered the outer space of the composite microbubble. DOX was loaded on GO by $\pi-\pi$ conjugate action, and FA was coupled on the surface of GO through amidation reaction. In addition, the loading rates of DOX and GO in the obtained FA/DOX/GO/DOX/PLA microbubbles were respectively 7.42 and 19.56% in the previous study.[14]

Figure 2 shows the particle distribution and zeta potential of composite microbubbles. From Figure 2a, the particle size distribution of composite microbubbles showed a single peak at about 600 nm and conformed to the injection standard. Figure 2b shows that the zeta potential of composite microbubbles is about (-37.5 ± 10) mV, which made them difficult to precipitate or agglomerate, and the obtained composite microbubbles had good stability.

2.2. Antitumor Activity in Vitro. *2.2.1. Inhibition Rate of MCF-7 Cells.* As shown in Figure 3, after the free DOX group, DOX/GO/PLA microbubbles, DOX/PLA microbubbles, DOX/GO/DOX/PLA microbubbles, and FA/DOX/GO/DOX/PLA microbubbles interacted with breast cancer cells MCF-7 in the same order for 48 h; the inhibition effect of every group of microbubbles on breast cancer cells MCF-7 obviously increased with the increase of drug concentration, which obviously showed a dose-dependent phenomenon. There was no obvious difference between the DOX/GO/PLA microbubble group and free DOX group; the existence form of DOX loading on GO in DOX/GO/PLA microbubbles was similar to that of the free DOX group

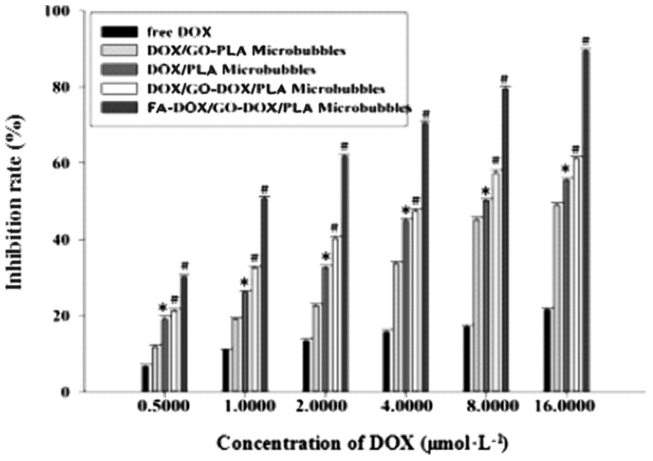

Figure 3. Inhibition rate of MCF-7 cells after the drug treatment for 48 h in each group ($n = 6$); note: vs free DOX, $^{\#}P < 0.01$, $^{*}P < 0.05$.

because of the $\pi-\pi$ conjugate effect between the DOX and GO. However, the cell inhibition rate of the PLA/DOX microbubble group had significant difference in comparison with the free DOX group, and the obtained data were statistically significant ($^{*}P < 0.05$), which indicated that the effect of microbubbles enveloping the DOX on the drug loading was favorable. Similarly, compared with the free DOX group, the cell inhibition rates of the DOX/GO/DOX/PLA microbubble group and FA/DOX/GO/DOX/PLA microbubble group also had significant differences, and $^{*}P < 0.01$. Furthermore, the difference of cell inhibition rates between the DOX/GO/DOX/PLA microbubble group and FA/DOX/GO/DOX/PLA microbubble group was obvious and there was statistical significance ($^{*}P < 0.05$), suggesting that the FA on the composite microbubbles was conducive to its targeting in combination with the breast cancer cell MCF-7 receptor. Thus, it could be seen that the prepared FA/DOX/GO/DOX/PLA microbubbles had satisfying targeting and inhibition effects on breast cancer cells MCF-7. In addition, for DOX/PLA microbubbles, DOX/GO/DOX/PLA microbubbles, and FA/DOX/GO/DOX/PLA microbubbles, their tumor inhibition rates were all higher than that of the free DOX group, which was because the DOX being loaded inside the microbubble and on the GO increased the drug capacity of

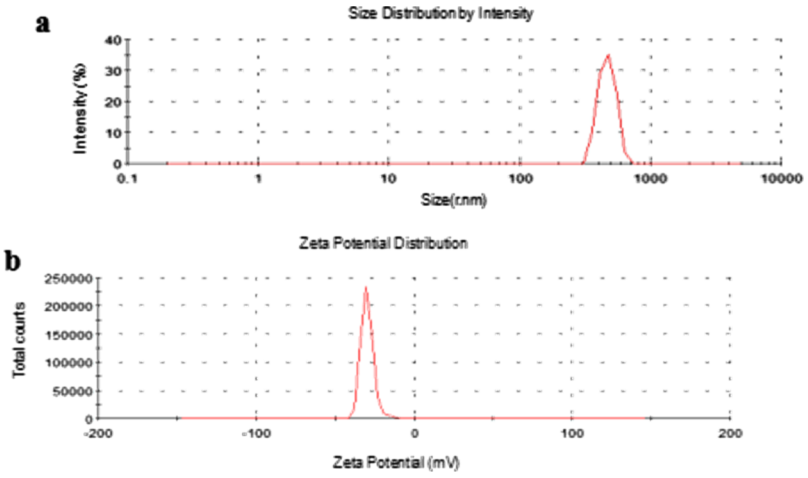

Figure 2. Particle distribution (a) and zeta potential (b) of the FA/DOX/GO/DOX/PLA microbubbles.

DOI: 10.1021/acsomega.8b03403
ACS Omega 2019, 4, 4691−4696

composite microbubbles and microbubbles encasing DOX avoided the burst release phenomenon of the drug.

2.2.2. MCF-7 Cell Activity. Figure 4 shows the MCF-7 cell activity by acridine orange (AO) staining in each experimental

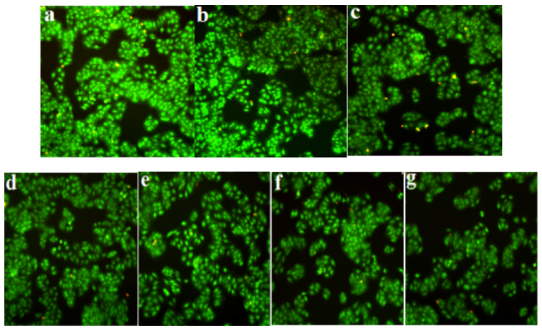

Figure 4. Activity of cells in each group: (a) control group, (b) blank GO/PLA microbubble group, (c) free DOX group, (d) DOX/GO/PLA microbubble group, (e) DOX/PLA microbubble group, (f) DOX/GO/DOX/PLA microbubble group, and (g) FA/DOX/GO/DOX/PLA microbubble group.

group. AO and intracellular DNA has a strong affinity, and their combination appears light green. It could be seen from Figure 4a,b, for the control group and the blank GO/PLA microbubble group, the growth state of cells were good, the cells were plump, and the nuclei were bright green, indicating that the DNA synthesis of the cells was active. It can be seen that the carrier used (GO/PLA) in the experiment has no obvious cytotoxicity on breast cancer cells MCF-7. As shown in Figure 4c–g, the free DOX, DOX/GO/PLA microbubble group, DOX/PLA microbubble group, DOX/GO/DOX/PLA microbubble group, and FA/DOX/GO/DOX/PLA microbubble group all had inhibitory effects on cell activity. The number of cells decreased, the growth state was poor, the morphology was slightly irregular, and the nuclear color was weakened. Compared with other groups, the FA/DOX/GO/DOX/PLA microbubble group had the most inhibitory effect on cells: the number of cells was significantly reduced, the edge of cells was blurred, and the color of nucleus was weakened. This was because the FA/DOX/GO/DOX/PLA microbubble group added the targeting factor and could specifically combine with the FA receptors, which increased the number of FA/DOX/GO/DOX/PLA microbubbles around the cells; the increase of the amount of drugs entering cells resulted in improvement in the inhibition rate of tumor cells.

2.3. Acute Toxicity Test. After intraperitoneal injection of composite microbubbles, the mice for the composite microbubble group of 52.389 mg·kg^{-1} showed a decrease in activity and diet and water consumption, but there was no death observed. For the injection group of 65.486 mg·kg^{-1}, the activity of mice and their weight reduced, they ate less and drank less, and one died. For the injection group of 81.858 mg·kg^{-1}, mice showed convulsions and weight loss, and three died. For the injection group of 102.322 mg·kg^{-1}, the activity of mice decreased, and they presented shaking spasms and ataxia, and eight died. All mice in the injection group of 127.903 mg·kg^{-1} died.

The mice death records after injecting composite microbubbles are shown in Table 1. The median lethal dose (LD_{50}) is calculated by using the Karber method, and LD_{50} was 87.529 mg·kg^{-1}. The confidence interval of 95% was 74.245–103.188

Table 1. Results of the Mice Death Records after Injecting Composite Microbubbles (n = 10)

group	dose (mg·kg^{-1})	death number	death rate (%)
1	52.389	0	0
2	65.486	1	10
3	81.858	3	30
4	102.322	8	80
5	127.903	10	100

mg·kg^{-1}. Results showed that when the dose of microbubbles was less than 65.486 mg·kg^{-1}, mice did not show the acute toxicity phenomenon. In the application of ultrasound imaging, PLA composite microbubbles of 40 mg·kg^{-1} were adopted, which indicates that prepared UCA microbubbles have satisfactory biosafety.

2.4. Ultrasound Imaging in Vitro. In vitro ultrasound imaging effects of the physiological saline, DOX/PLA microbubbles, GO/PLA microbubbles, and FA/DOX/GO/DOX/PLA microbubbles are shown in Figure 5a–d. Figure 5a

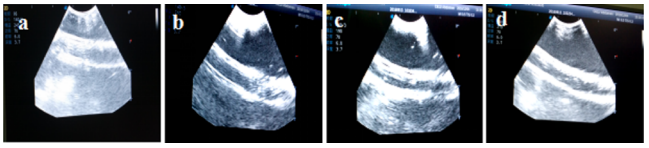

Figure 5. In vitro ultrasonic imaging effects of (a) physiological saline group, (b) DOX/PLA microbubble group, (c) GO/PLA microbubble group, and (d) FA/DOX/GO/DOX/PLA microbubble group.

shows that the imaging of the silicone tube was blurred because of the lower echo in the physiological saline group. As shown in Figure 5 b–d, the echo effects of the DOX/PLA microbubble group, GO/PLA microbubble group, and FA/DOX/GO/DOX/PLA microbubble group enhanced and their contrast effects remarkably improved in comparison with those of the physiological saline group. The results showed that the addition of FA/GO and DOX did not affect the ultrasonic imaging effect of the PLA microbubbles, and the obtained FA/DOX/GO/DOX/PLA microbubbles have excellent ultrasonic imaging characteristics in vitro.

2.5. Ultrasound Imaging in Vivo. The ultrasound enhancement effect of PLA composite microbubbles in major organs of the animal body is shown in Figure 6. Figure 6a shows the imaging effect on rabbit heart before and after intraperitoneal injection of composite microbubbles. Before the injection, left and right ventricular imaging was pale because the blood echo was lower, and as a result, the left and right atria could not be presented in ultrasonic imaging. After injection, ultrasound imaging of both left and right ventricles became clear because of the strong echo of composite microbubbles under the ultrasound action. Additionally, the ultrasonic imaging showed that composite microbubbles first appeared in the right atrium and the right ventricle and then the left ventricle and the left atrium. Figure 6b shows the ultrasonic imaging effect on rabbit thymus before and after the injection of PLA composite microbubbles. Before injection, ultrasound imaging showed low contrast and blurred outline in rabbits. After injection, the ultrasonic imaging effect on rabbit thymus was obvious, and its outline was clear. Figure 6c shows the imaging effect on rabbit liver before and after the injection of PLA composite microbubbles. The echo signals of the hepatic vein, the portal vein, and the inferior vena cava in

DOI: 10.1021/acsomega.8b03403
ACS Omega 2019, 4, 4691–4696

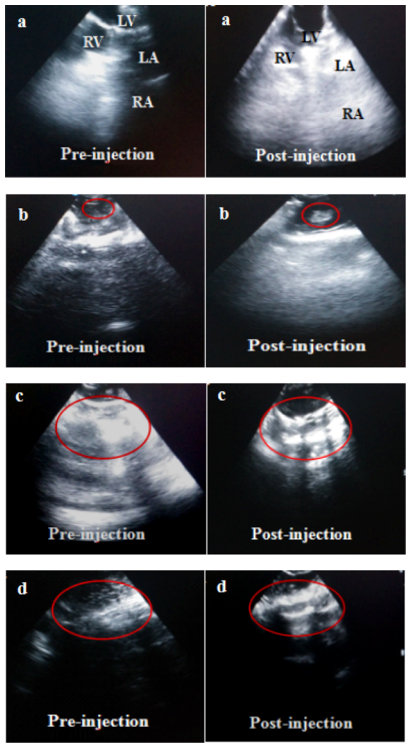

Figure 6. Ultrasonic imaging of rabbits before and after injecting FA/DOX/GO/DOX/PLA microbubbles: (a) heart, (b) thymus, (c) liver, and (d) kidney.

rabbit liver were not clear before injection, but they were obviously enhanced after injection. Ultrasonic imaging effect on rabbit kidney before and after the injection of PLA composite microbubbles is shown in Figure 6d. The echo signal was weak in the field of vision; the kidney boundary was not clear before injection. After injection, there was a stronger echo under the ultrasound effect; the kidney was fully perfused and its boundary enhancement was clear, and the ultrasonic imaging enhanced obviously. To sum up, the ultrasound imaging effects of PLA composite microbubbles in solid organs such as the heart, thymus, liver, and kidney of New Zealand rabbits were strong, which was helpful in diagnosis and treatment.

The prepared composite microbubbles had good ultrasound imaging effect and would be able to safely cycle in the body. The vital signs of the rabbit were stable during the process of imaging. There were no harmful responses observed, even after imaging .

3. CONCLUSIONS

In this study, FA/DOX/GO/DOX/PLA microbubbles were constructed based on the following three points: (1) DOX is a broad-spectrum antineoplastic drug which can kill breast cancer cells. It can form a $\pi-\pi$ conjugation effect with GO. (2) GO is a new biosafety carrier material which can increase the therapeutic effect by loading DOX and linking FA. (3) The FA receptor is a high-expression receptor of the breast cancer cell surface, and the targeting factor FA can specifically combine with the FA receptor and does not affect normal cells. The new PLA composite microbubbles showed excellent targeting and therapeutic effects on breast cancer cells MCF-7 and clear ultrasound imaging.

4. MATERIALS AND METHODS

4.1. Reagents and Materials. Graphite powder (Lutang graphite-processing plant in Chenzhou of Hunan province, China); nitrogen (liming gas factory in Harbin, China); FA and hydrochloric acid DOX (Dalian Mellon Biological Technology Co., Ltd, China); PLA, methylene chloride, absolute ethyl alcohol, PVA, and isopropyl alcohol (analytical pure, Tianjin Kemio Chemical Reagent Co., Ltd, China); ethyl-(3-2 methyl propyl) carbide imine hydrochloride and *N*-hydroxy succinimide (National Medicine Group Chemical Reagent Co., Ltd, China); dimethyl sulfoxide (Tianjin Solomon Biological Technology Co., Ltd, China); AO (Dalian Mellon Biological Technology Co., Ltd, China) were used; and saline is provided by the Jiamusi pet animal hospital.

Breast cancer cells MCF-7 (Shanghai Cell Bank in the Chinese Academy of Sciences); CCK8 kit (DOJINDO, Japan); 96 cell culture plate, cell culture bottle, and 6 cell culture plate (CoStar company, US); fetal bovine serum (Gibco company, US); Dulbecco's modified Eagle's medium (DMEM), penicillin, streptomycin, and cell digestive liquid of pancreatic enzyme (Hyclone company, US); SPF KM mice (Harbin Medical University, China); and New Zealand white rabbit were used.

4.2. Instruments. The following instruments were used: a table centrifuge (TGL-16G, Shanghai Anting Science Instrument Factory, China); ultrasonic cell disrupter (JY92-2D, Ningbo Xinzhi Biological Technology Co., Ltd, China); scanning electron microscope (ZSM-6360LV, Nanjing University Instrument Factory, China); TEM (JEM-1200EX, JEOL Co., Ltd, Japan); vacuum freeze drier (AD2OFL, Beijing Xinmozhen Technology Co. Ltd, China); nanoparticle size analyzer (Zetasizer Nano-ZS90, Malvern Instrument Co., Ltd, UK); enzyme standard instrument (RS232, Shanghai Masa Biotechnology Co., Ltd, China); inverted microscope (V-LH50HG, Tokyo Olympus Co., Ltd, Japan); low-temperature high-speed centrifuge (TD24-WS, Hunan Xiangyi Laboratory Instrument Development Co., Ltd, China); and Doppler color ultrasound imaging system (S40, Wuhan Liang Kang Medical Device Co., Ltd, China).

4.3. Preparation of Targeting Drug-Loaded PLA Composite Microbubbles. GO was prepared by using natural graphite powder as the starting material with Hummer's method.[13] PVA was heated and dissolved in distilled water to obtain PVA solution with a concentration of 3.5% and mixed with the proper amount of GO, and then, the PVA was covalently grafted onto GO, and GO/PVA compound was obtained by the esterification reaction.

A certain amount of DOX was added into the PLA methylene chloride solution of 0.060 g·mL^{-1}; then, N_2 was introduced into the above system, treating with the ultrasonic probe at 120 W, and the primary emulsion was formed. The primary emulsion was added to a certain amount of the water-dispersing system of the GO/PVA compound, and the multiple emulsion was formed through ultrasound emulsification under 210 W; then, isopropyl alcohol solution of 5.5% was added into the multiple emulsion, and the reaction was sustained for 2.5 h under magnetic stirring at room temperature. After centrifugal washing, the PLA microbubbles encasing DOX inside and loading GO on the surface (GO/DOX/PLA) were obtained. A certain amount of DOX was added into the above system again and stirred under dark condition at room temperature, followed by centrifugal

DOI: 10.1021/acsomega.8b03403
ACS Omega 2019, 4, 4691−4696

washing; DOX was loaded on the GO in GO/DOX/PLA microbubbles, and DOX/GO/DOX/PLA microbubbles were obtained. Finally, to link the targeting factor onto the microbubbles, FA solution was added into the obtained DOX/GO/DOX/PLA microbubbles, and they reacted under the activation effect of *N*-hydroxy-succinamide and carbonated diimide hydrochloride at room temperature and in a dark environment; the targeted drug-loaded PLA composite microbubbles (FA/DOX/GO/DOX/PLA) were obtained after vacuum freeze-drying.

Blank GO/PLA microbubbles, DOX/GO/PLA microbubbles, DOX/PLA microbubbles, and DOX/GO/DOX/PLA microbubbles were also prepared according to the above method.

4.4. Antitumor Activity in Vitro. *4.4.1. Cell Culture.* DMEM containing 10% fetal bovine serum and 1% penicillin−streptomycin was used to cultivate breast cancer cells MCF-7 under fully saturated humidity and 5% CO_2 (v%) at 37 °C. In addition, cells were washed 1−2 times with phosphate-buffered saline (PBS) solution (pH = 7.4) and digested with 0.25% trypsin. After breast cancer cells MCF-7 were cultivated two or three generations, the best cells in the logarithmic phase were selected for use.

4.4.2. Inhibition Rate of MCF-7 Cells by the CCK-8 Method. After breast cancer cells MCF-7 in the logarithmic growth phase were digested by trypsin, a single cell suspension was obtained and the cell number was calculated. Breast cancer cells MCF-7 with a concentration of 2×10^5 number·mL^{-1} were inoculated in a 96-well plate at 100 μL per well. Cells were incubated for 24 h, and the culture medium was replaced with the serum-free medium; starvation treatment was carried out for 12 h. A culture solution containing the drug without serum was added per well at a concentration of 0.5−16 μmol·L^{-1} and a volume of 100 μL per well. The blank well was added with an equal amount of normal culture. Cells were cultivated for 48 h at 37 °C and 5% CO_2, and then, 10 μL of CCK-8 solution was added to each well and incubated for 4 h. The absorbance of every well was measured at 450 nm by using an enzyme standard instrument, and the cell growth inhibition rate was calculated according to the following formula. SPSS17.0 statistical software was used to analyze the cell growth inhibition rate of each group, and *T* test and variance analyses were used for the comparison of the different drug administration groups. $^*P < 0.05$ indicated that the difference was significant.

$$\text{Inhibition rate (\%)} = (\text{mean value of OD in the control group} - \text{mean value of OD in the drug group})/\text{mean value of OD in the control group} \times 100\%$$

4.4.3. Observation of Cell Activity by AO Staining. Breast cancer cells MCF-7 in the logarithmic growth phase were digested with trypsin to prepare a single cell suspension, and cell counts were performed. Breast cancer cells MCF-7 with a concentration of 2×10^5 number·mL^{-1} were inoculated onto a 6-pore plate at 2 mL per well. Cells were normally cultivated at 37 °C, 5% CO_2 (v%), and fully saturated humidity. The cultivation process continued for 24 h until the cells were fully adhered to the plate. Then, the culture medium was removed and cells were divided into the control group and drug groups. Complete medium was added to the control group. In the drug groups, the prepared drug solution with the complete culture medium and different composite microbubbles were added to each well, and the DOX concentration in each well was 4 μmol·L^{-1}. After 4 days of incubation at 37 °C and 5% CO_2, a certain volume of AO solution was added into every well and the incubation process was sustained for 10−20 min. After removing the culture medium, cells were washed 2−3 times with PBS and photographed by using an inverted fluorescence microscope.

4.5. Acute Toxicity Test. All animal experiments in the study have received protocol approval from the Institutional Animal Protection and Use Committee of Jiamusi University. A total of 50 SPF KM mice were selected and randomly divided into 5 groups with 10 mice in each group. The composite microbubble suspensions at concentrations of 52.389, 65.486, 81.858, 102.322, and 127.903 mg·kg^{-1}, respectively, were injected into the abdominal cavity of each group of mice. Then, acute toxicity reaction and mortality of mice were observed under continuous observation for 7 days; the Karber method was used to calculate the value of LD_{50}.

4.6. Ultrasound Imaging in Vitro. Before the experiment, an appropriate amount of distilled water was degassed for use. With the transparent elastic silicone tube (medical grade) as the external model of the blood vessel, the degassed water was slowly poured into the water tank; the elastic silicone tube was placed under the water tank surface. The ultrasonic probe was submerged under the liquid surface and faced the silicone tube. Using saline as a blank control group, a certain amount of FA/DOX/GO/DOX/PLA microbubbles was dispersed in the physiological saline, and then, the physiological saline and the FA/DOX/GO/DOX/PLA microbubbles were separately injected into the silicone tube. The longitudinal and transverse sections of the rubber tube were observed by pulse-inversion harmonic imaging using the Doppler color ultrasound imaging system.

4.7. Ultrasound Imaging in Vivo. A New Zealand white rabbit was anesthetized, and its abdomen was depilated. The peripheral venous channel in the marginal vein of rabbit ear was identified. A certain concentration and dose of composite microbubbles were injected through the vein of rabbit ear, followed by washing with a proper amount of saline. The Doppler color ultrasound imaging system was employed to observe and record the echo intensity of the heart, thymus, liver, and kidney of the rabbit. Experiments were conducted in a generally acceptable ethical and humane fashion.

AUTHOR INFORMATION

Corresponding Authors

*E-mail: zjie612@163.com (J.Z.).
*E-mail: zhshj2003@163.com (S.Z.).

ORCID

Jie Zhang: 0000-0002-4257-696X

Notes

The authors declare no competing financial interest.

ACKNOWLEDGMENTS

This work was supported by the National Natural Science Foundation of China (no. 81601616), the Science Foundation of Heilongjiang Province (no. H2016086) and the Scientific Research Project of Jiamusi University (no. XZYF2018-42), excellent innovation team based on the basic scientific research

DOI: 10.1021/acsomega.8b03403
ACS Omega 2019, 4, 4691−4696

vocational cost for the provincial undergraduate universities in Heilongjiang.

REFERENCES

(1) Parkin, D. M.; Pisani, P.; Ferlay, J. Global cancer statistics. *Ca-Cancer J. Clin.* **1999**, *49* (1), 33−64.

(2) Giordano, S. B.; Gradishar, W. Breast cancer. *Curr. Opin. Obstet. Gynecol.* **2017**, *29*, 12.

(3) Klibanov, A. L. Ligand-Carrying Gas-Filled Microbubbles: Ultrasound Contrast Agents for Targeted Molecular Imaging†. *Bioconjug. Chem.* **2005**, *16*, 9−17.

(4) Hölscher, T.; Sattin, J. A.; Raman, R.; et al. Real-time cerebral angiography: sensitivity of a new contrast-specific ultrasound technique. *AJNR Am J Neuroradiol.* **2007**, *28*, 635−639.

(5) Vicenzini, E.; Delfini, R.; Magri, F.; et al. Semiquantitative Human Cerebral Perfusion Assessment With Ultrasound in Brain Space-Occupying Lesions. *J. Ultrasound Med.* **2008**, *27*, 685−692.

(6) Meyer-Wiethe, K.; Seidel, G.; et al. Ultrasound cerebral perfusion analysis based on a mathematical model for diminution harmonic imaging. *Methods Inf Med.* **2007**, *46*, 308−313.

(7) Blohmer, J. U.; Reinhardt, M.; Schmalisch, G.; et al. Video-densitometry in the examination of focal breast lesions after injection of an ultrasound contrast agent. *Anticancer Res* **2006**, *26*, 1691−1698.

(8) Liu, Z.; Guo, J.; Wang, S.; et al. Evaluation of transabdominal ultrasound after oral administration of an echoic cellulose-based gastric ultrasound contrast agent for gastric cancer. *BMC Canc.* **2015**, *15*, 932.

(9) Molinari, F.; Eichinger, M.; Risse, F.; et al. Accurate and automatic carotid plaque characterization in contrast enhanced 2d ultrasound images. *Conference proceedings IEEE Engineering in Medicine and Biology Society*, 2007; pp 335−338.

(10) Xing, W.; Zhigang, W.; Bing, H.; et al. Targeting an Ultrasound Contrast Agent to Folate Receptors on Ovarian Cancer Cells. *J. Ultrasound Med.* **2010**, *29*, 609−614.

(11) Testa, A. C.; Timmerman, D.; Exacoustos, C.; et al. The role of CnTI-SonoVue in the diagnosis of ovarian masses with papillary projections: a preliminary study. *Ultrasound Obstet. Gynecol.* **2007**, *29*, 512−516.

(12) Huang, P.; Xu, C.; Lin, J.; et al. Folic Acid-conjugated Graphene Oxide loaded with Photosensitizers for Targeting Photodynamic Therapy. *Theranostics* **2011**, *1*, 240−250.

(13) Hummers, W. S.; Offeman, R. E. Preparation of Graphitic Oxide. *J. Am. Chem. Soc.* **1958**, *80*, 1339.

(14) Zhao, Y.; Zhang, J.; Chang, C. Y.; et al. Preparation of Targeted and Drug-loaded PLA Composite Microbubble Ultrasound Contrast Agent. *Guangdong Chem. Ind.* **2017**, *44*, 22−23.

DOI: 10.1021/acsomega.8b03403
ACS Omega 2019, 4, 4691−4696